Experimental Ultraviolet (UV) photooxidation of ferrous iron and carbonate bearing solutions as an analog for sunlit water bodies on early Mars. V.B. Rivera Banuchi[1], J. Gong[2], J.A. Hurowitz[1], and T. Bosak[2], [1]Stony Brook University, Stony Brook, NY, 11794, [2]Massachussetts Institute of Technology, Cambridge, MA, 02139.

Introduction: UV photooxidation of ferrous iron has been suggested as a potentially important mechanism of oxidation and mineralization for early Martian surface aqueous environments. UV photooxidation has been invoked as a contributor to the formation of jarosite-hematite deposits in Meridiani Planum [1,2], as well as the redox stratification inferred from variations in iron mineral abundances in sedimentary rocks in Gale Crater [3]. An understudied component of previous Mars-focused UV photochemistry studies is the influence of dissolved inorganic carbon (DIC) in solution, which is an expected component of solutions under the high pCO_2 atmosphere of early Mars. In this study, we examine UV photooxidation of sealed ferrous iron (1.79 mM) and DIC (35.0 mM) bearing solutions under anoxic conditions at varying initial pH conditions to understand what effect DIC has on Fe photooxidation efficacy.

Experimental Setup: UV irradiation experiments were conducted with a 450 W medium pressure Hg lamp within an enclosed cabinet. Iron carbonate solutions were prepared within a Coy anoxic glovebox and placed within a sealed fused quartz Erlenmeyer flask before irradiation. Initial and final solution samples were collected to measure Fe concentration, pH, and temperature. Solutions were acidified on the same day that they were collected for total Fe concentration measurements. The flask has a sampling arm for the collection of gas samples during irradiation. To ensure that gas sample measurements were not impacted by residual N_2-H_2 headspace gas from the glovebox atmosphere, some of the experiments included purging the flask headspace with ultra-high purity (UHP) N_2 gas prior to sample irradiation.

Results: *Solution Chemistry*. Temperature was measured once the solutions were returned to the anoxic glovebox; the maximum solution temperature after irradiation was 35.3°C. On average, the measured pH of the final solutions was ~0.29 pH units higher than their initial pH values (**Fig.1A**), and iron concentration changes ranges from ~0.1 ppm to ~10 ppm. A model of the effects of Fe photooxidation from initial pH values ranging from pH 4-7 (**Fig.1B**, black lines) based on reaction stoichiometry:

(1) $Fe^{2+}+H_2O+h\nu=Fe^{3+}+OH^-+0.5H_2$

indicates that for experiments in which iron concentration changes were <4 ppm, changes in solution pH and Fe concentration can be explained by UV photooxidation. For experiments with iron concentration changes >4ppm, the photooxidation model does not adequately explain the combination of pH change and Fe concentration change; however, if we consider the following reactions:

(2) $Fe^{3+}+3H_2O=Fe(OH)_3+3H^+$

(3) $3HCO_3+3H^+=H_2CO_3$

then it is possible to imagine that in cases where iron loss was more significant, some amount of hydrolysis and pH buffering by bicarbonate would result in vertical migration of data points on **Fig.1B** (green line). Pure hydrolysis (rxn 2) without buffering is shown by orange lines on **Fig.1B** for initial pH values of 4 and 7. CO_2 degassing would result in increased pH (negative change on X-axis) with no change in iron concentration. In one case, iron concentration increased between initial and final measurements; we attribute this to a sample contamination or analysis issue unrelated to Fe behavior during irradiation.

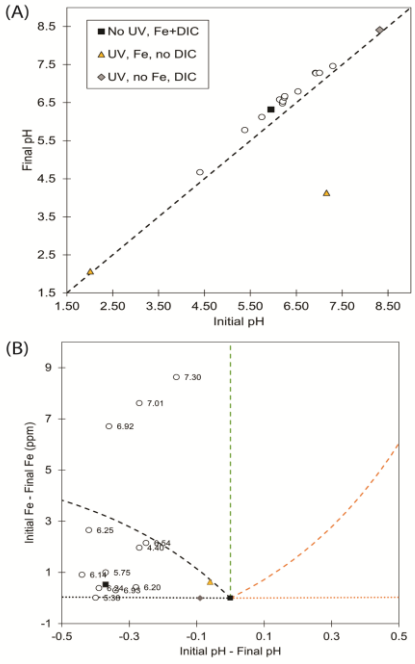

Fig. 1A: Measured initial and final pH values for photooxidation experiments. **1B**: Change in pH and Fe-concentration between initial and final measurements. Black dotted and dashed lines: change in pH and Fe concentration due to photooxidation for $pH_{initial}$ = 7 and 4, respectively; Orange dotted and dashed lines: change in pH and Fe concentration due to hydrolysis for $pH_{initial}$ = 4 and 7, respectively; Green dashed line, change in pH and Fe concentration due to hydrolysis and buffering.

Mineralogy. UV irradiation experiments that had a solution color change after irradiation were $pH_{initial}$ 5.38, 6.14, 6.25, 6.54, 6.92, 6.93, 7.01, and 7.30, likely

due to some phases precipitating. These generally yielded insufficient solid for X-Ray Diffraction (XRD) analysis, but in few cases, we were able to filter enough material. These XRD patterns had high background, potentially caused by amorphous phases. The sample from the $pH_{initial}$ 7.01 experiment yielded sufficient sample for a low resolution pattern with peaks characteristic of goethite. Attenuated total reflectance-Fourier transform reflectance spectroscopy (ATR-FTIR) was conducted for both solid and solid-liquid samples to assess general mineralogy of irradiation products. Samples from experiments $pH_{initial}$ 6.25 and 6.92 contained IR absorption bands characteristic of siderite/chukanovite (Fe-carbonates) and goethite.

Gaseous Phases. Headspace samples were collected during UV irradiation at 0, 30, 90, 150, and 180 minutes. Hydrogen and methane gas were present in each experiment. Glovebox atmosphere samples were collected in order to understand if the produced hydrogen gas was greater than any H_2 contributed from the glovebox. All of the hydrogen gas produced was less than the maximum that could have been contributed from the glovebox, which was 0.0295 atm (**Fig.2A**). Methane was also present in the glovebox atmosphere measurements (0.00143 atm), but the $pH_{initial}$ 6.92 and 7.01 experiments yielded CH_4 abundances higher than this value (**Fig.2B**). Work is ongoing to understand whether these increased CH_4 measurements are statistically significant.

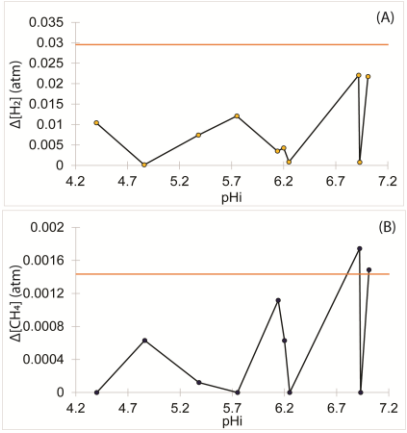

Fig.2A: Hydrogen gas produced during irradiation versus initial pH conditions. Orange solid line represents the amount of H_2 that could originate from the glovebox. **2B**: Methane gas produced during irradiation versus initial pH conditions. Orange solid line represents the concentration of CH_4 measured from glovebox samples.

Discussion: The UV irradiation of Fe-DIC solutions appears to be inefficient across a range of pH conditions. The extent of iron loss was minimal and, in the experiments conducted, there was an overall increase in this loss at higher initial pH, although inconsistent when comparing experiments $pH_{initial}$ 6.92 and 6.93. UV photooxidation of aqueous iron is minimized when DIC is present at the concentrations modeled for a surficial water body under a 1 bar CO_2 atmosphere [4]. The mineralogical data for these experiments is minimal due to the lack of significant iron loss. Of note is the identification of iron carbonate (siderite/chukanovite) at pHi 6.25 and 6.92 as this phase has remained elusive on the Martian record (e.g., [5]). Hydrogen produced with irradiation was somewhat greater with initial higher pH conditions, although again inconsistent in experiments pHi 6.92 and 6.93. Overall, hydrogen gas production was minimal in these experiments. The lack of hydrogen production is due to DIC content in the solutions, a finding consistent with Dodd et al. (2022) who found that an increase of 5mM DIC led to a 60x reduction H_2 production [6]. Hydrogen has been invoked as a potential greenhouse gas for early Mars [7] so understanding how DIC affects this yield from iron carbonate systems is essential. The presence of methane, although minimal, appears to be unrelated to the presence of UV radiation as it was identified in pre-UV samples. For methane, there is also no correlation to initial pH conditions. Overall, the lack in significant chemical changes in these experiments may suggest that Fe-DIC complex formation in solution may prevent significant iron UV photooxidation. Future work will assess iron UV photooxidation reaction rate and speciation under these chemical conditions.

References: [1] Hurowitz, J.A. et al. (2010) *Nat. Geo*., 3(5), 323-326. [2] Nie, N.X. et al. (2017) *EPSL*, 458, 179-191. [3] Hurowitz, J.A. et al. (2017) *Science*, 356(6341). [4] Tosca, N.J. and McLennan, S.M. (2009) *Geo. Cos. Ac*., 73(4), 1205-1222. [5] Ehlmann, B.L. et al. (2008) *Science*, 322(5909), 1828-1832. [6] Dodd, M.S. et al. (2022) *EPSL*, 584, 117469. [7] Tosca, N.J. et al. (2018) *Nat. Geo*., 11(9), 635-639.